Supporting information

A practical non-enzymatic urea sensor based on NiCo2O4nanoneedles

Sidra Amin[1,2,3], Aneela Tahira[1], , Amber Solangi[2], Valerio Beni[5], J.R. Morante[4], Xianjie Liu[6], Mats Falhman[6], Raffaello Mazzaro[1], Zafar Hussain Ibupoto[1,7]*, Alberto Vomiero[1]*

[1] Division of Materials Science, Department of Engineering & Mathematics, Luleå University of Technology, 97187 Luleå, Sweden
[2] National Centre of Excellence in Analytical Chemistry, University of Sindh, Jamshoro 76080, Pakistan
[3] Department of Chemistry, Shaheed Benazir Bhutto University, Shaheed Benazirabad 67450, Sindh Pakistan
[4] Catalonia Institute for Energy Research (IREC), Jardins de les Dones de Negre 1, Sant Adrià del Besòs, Barcelona 08930, Catalonia, Spain
[5]RISE Acreo, Research Institute of Sweden, Norrköping, Sweden
[6] Linköping University, Department of Physics, Chemistry and Biology, Surface Physics and Chemistry. Linköping University, Faculty of Science & Engineering.
[7] Institute of Chemistry, University of Sindh, Jamshoro76080, Sindh Pakistan

* Corresponding authors: Alberto Vomiero, Zafar Hussain Ibupoto
Email address. Alberto.vomiero@ltu.se, zafar.ibupoto@ltu.se

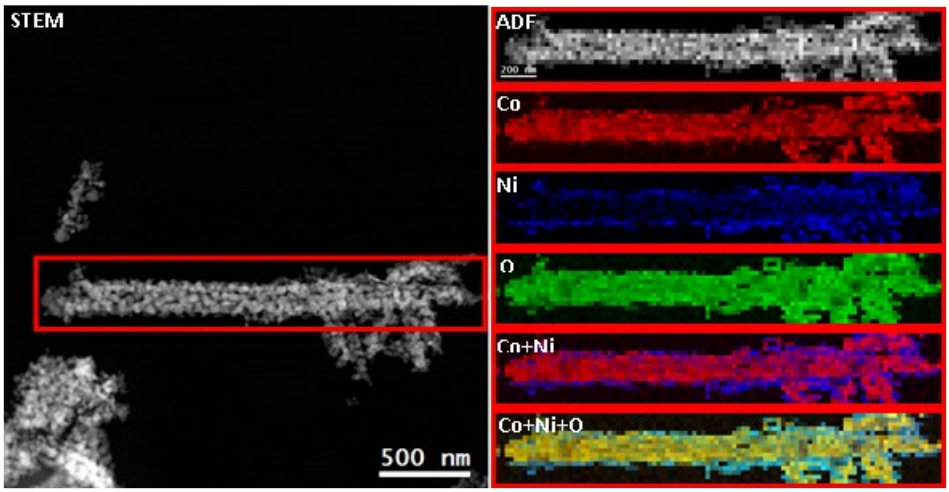

Figure S1. Low magnification EELS chemical composition maps of the $NiCo_2O_4$ nanoneedles obtained from the red rectangle area of the ADF-STEM micrograph. Individual Co (red), Ni (blue), O (green) maps and their composite

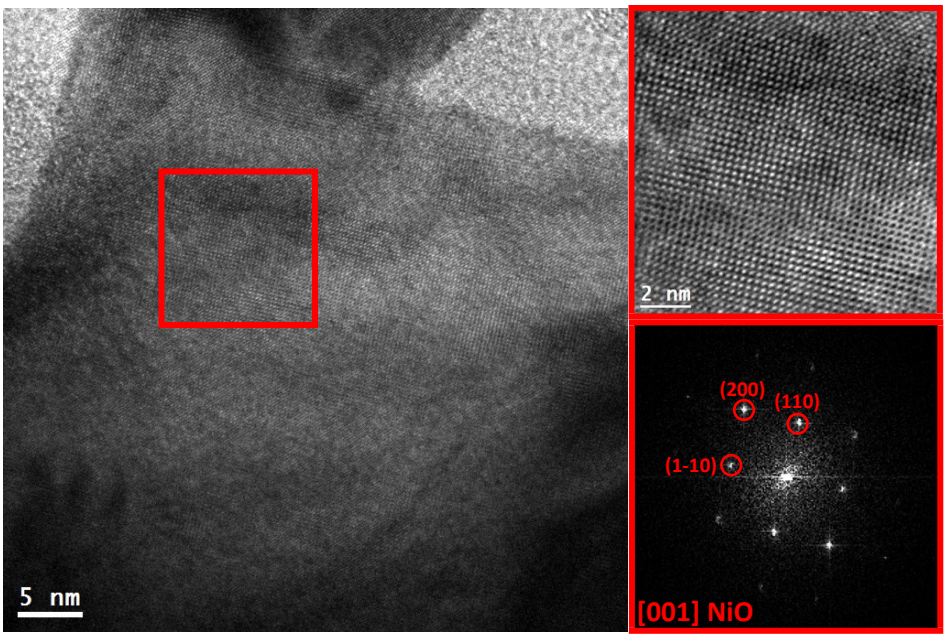

Figure S2. Left: HRTEM image of a nanoparticle from the $NiCo_2O_4$ nanoneedles. Right top: the HRTEM micrograph shows the detailed structure at the red squared region; Right bottom: the corresponding FFT spectrum indicates that the material crystallizes in the cubic NiO phase, [FM3-M]-Space group 225, with lattice parameters of a = b= c= 0.4179 nm, and $\alpha = \beta = \gamma = 90°$ as visualized along the [001] direction.

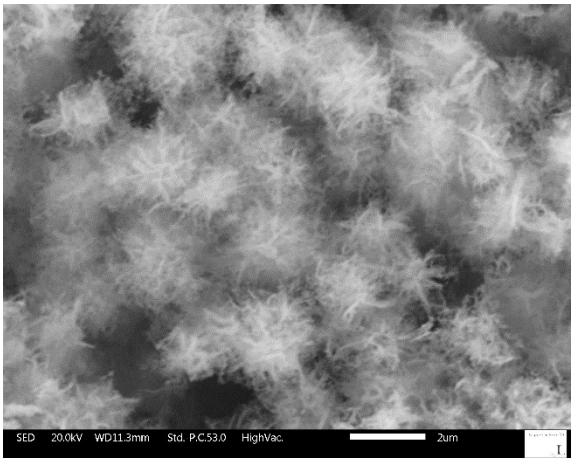

Figure S3. Low-resolution SEM image of the NiO flower-like structures

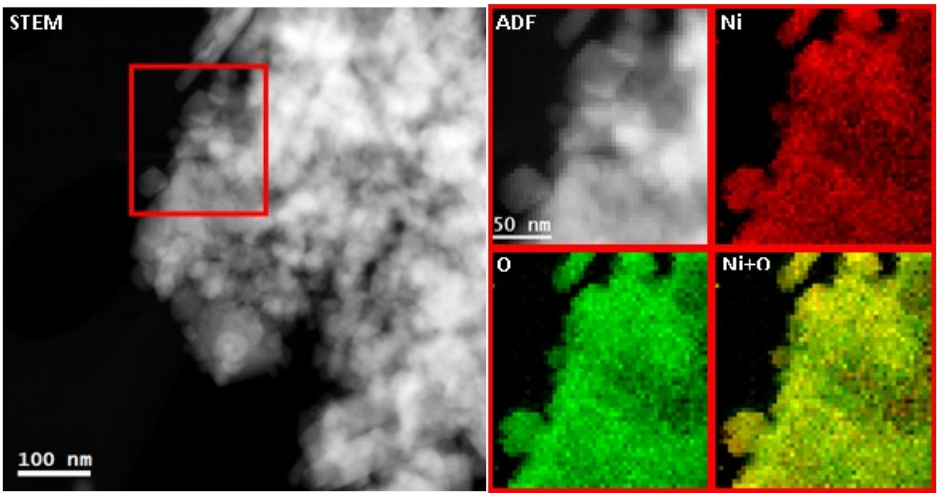

Figure S4. EELS chemical composition maps of the NiO nanostructures obtained from the red rectangled area of the ADF-STEM micrograph. Individual Ni (red), O (green) maps and their composite

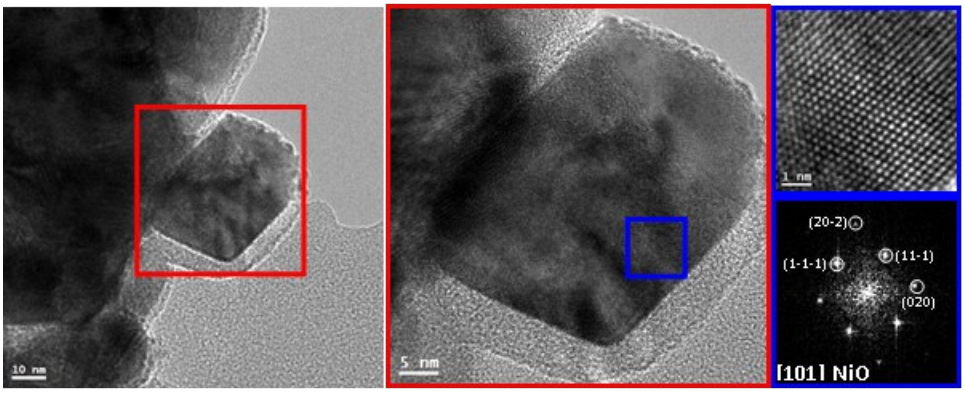

Figure S5. Left: Low magnification TEM image of the NiO nanostructures. Middle: HRTEM micrograph shows the structure of the nanoparticle located at the red squared region. Right: the atomically HRTEM of the blue squared region and the corresponding FFT spectrum indicates that the material crystallizes in the cubic NiO phase, [FM3-M]-Space group 225, with lattice parameters of a = b= c= 0.4179 nm, and $\alpha = \beta = \gamma = 90°$ as visualized along the [101] direction.

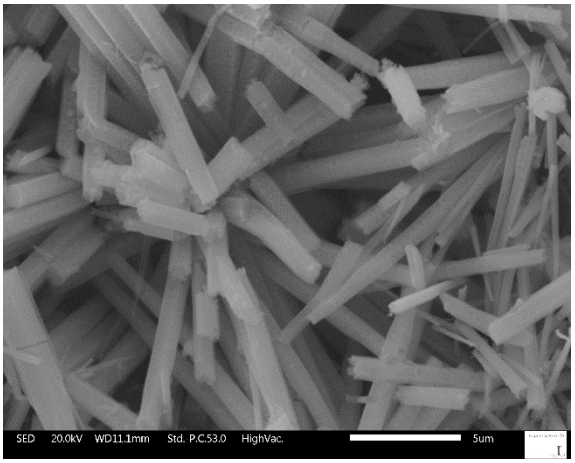

Figure S6. Low resolution SEM image of the Co_3O_4 nanostructures

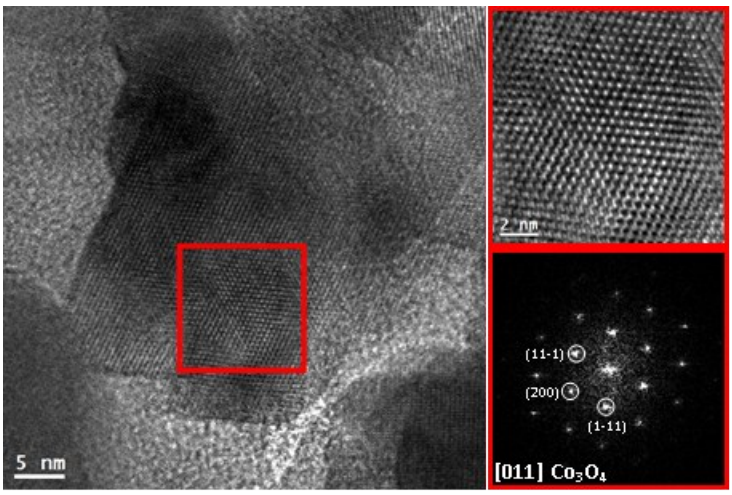

Figure S7. Left: HRTEM image of the Co_3O_4 nanostructures. Right: the atomically HRTEM of the red squared region and the corresponding FFT spectrum indicates that the material crystallizes in the cubic Co_3O_4 phase, [FM3-M]-Space group 225, with lattice parameters of a = b= c= 0.8065 nm, and $\alpha = \beta = \gamma = 90°$ as visualized along the [011] direction.

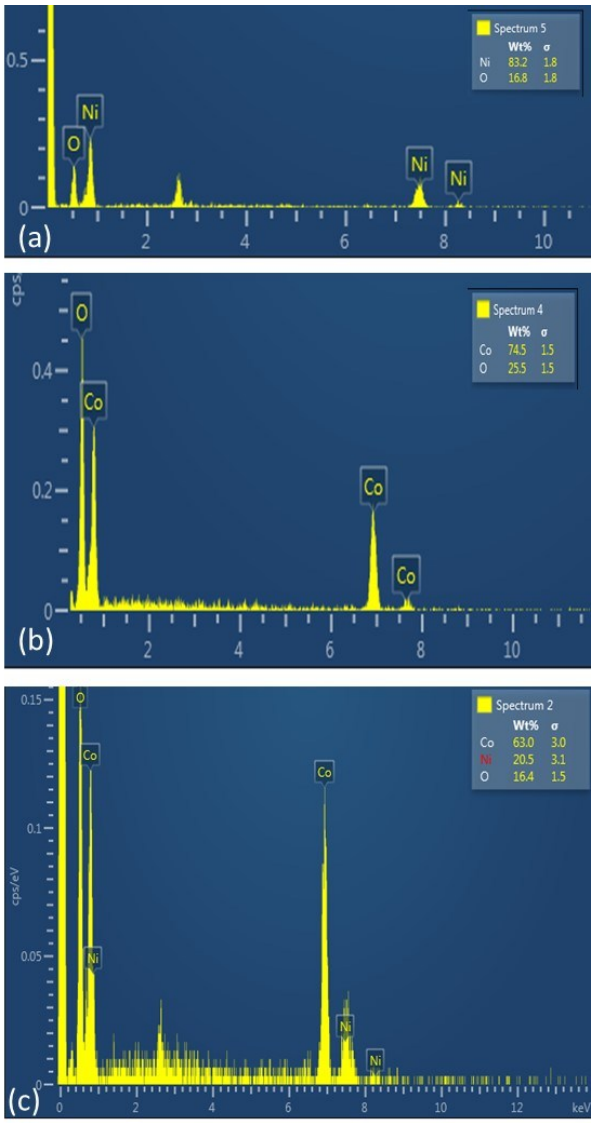

Figure S8: EDS analysis (a) NiO, (b) Co_3O_4, and (c) $NiCo_2O_4$ samples.

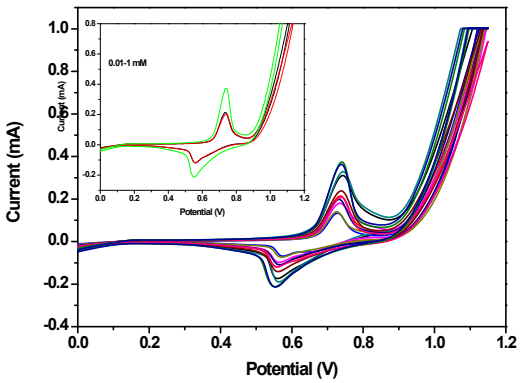

Figure S9. Cyclic voltammetry runs at different concentrations of urea: 0.01, 0.1, 1, 1.5, 2. 2.5, 3, 3.5, 4, 4.5, and 5 mM in 0.1M NaOH. The inset in the figure shows 0.01 – 1 mM in 0.1 M NaOH.

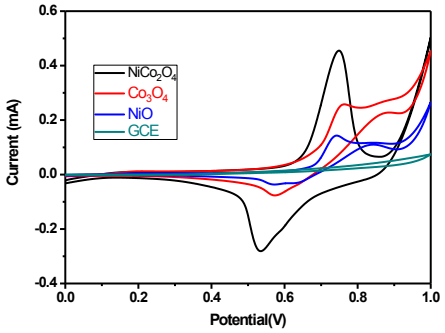

Figure S10. Comparison of GCE modified with different materials. Black line: $NiCo_2O_4$/GCE; red line: Co_3O_4/GCE; blue line: NiO/GCE.; blue green: GCE in the presence of 0.1mM urea solution.

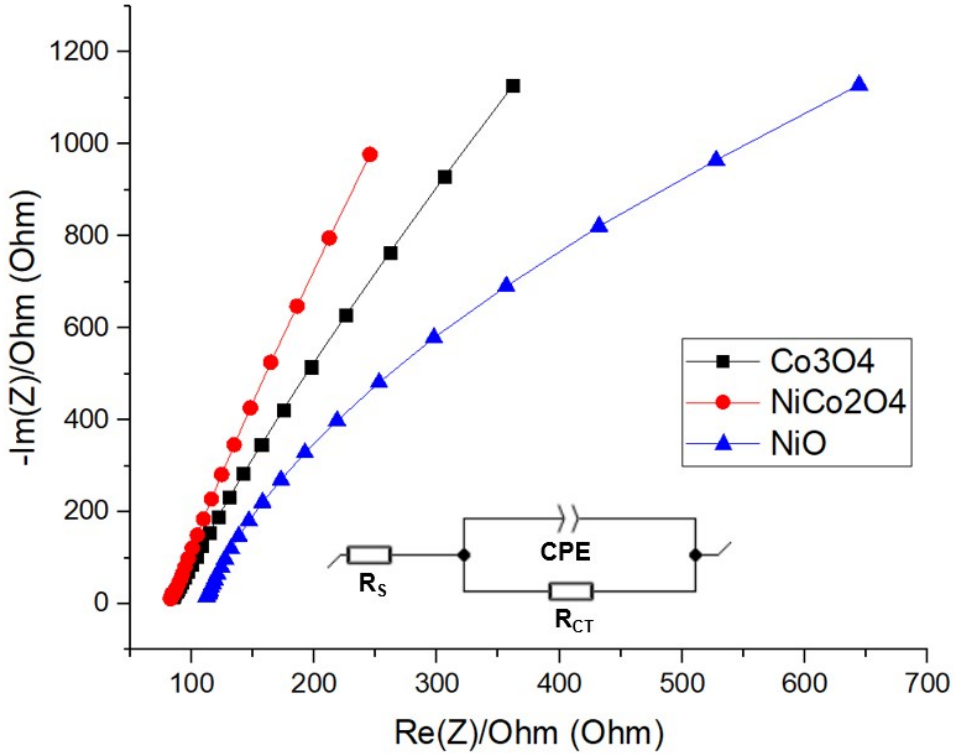

Figure S11. Nyquist plot of different materials at the bias potential of 200 mV and the amplitude of 10 mV and frequency range of 100 kHz to 100Hz at room temperature in 0.1M NaOH solution. The equivalent circuit used for the fitting of the curves is reported in the inset, with R_S, R_{CT} and CPE representing respectively the solution resistance, the charge transfer resistance (for residual faradaic processes) and a constant phase element.

The C_{DL} was calculated from the resulting values following this formula (cite McRory again):

$$C_{DL} = \left[Q_0 \left(\frac{1}{R_s} + \frac{1}{R_{ct}} \right)^{(a-1)} \right]^{1/a}$$

Where Q_0 and a are resulting from the CPE element fitting. The equivalent circuit components values are reported in table S1.

	R_s (Ω)	R_{CT} (Ω)	Q_0 (F cm^{-2})	a
NiO	109	4494	2.3050e-6	0.8878
Co3O4	82	23772	2.9230e-6	0.8783
NiCo2O4	82	51869	2.9130e-6	0.9069

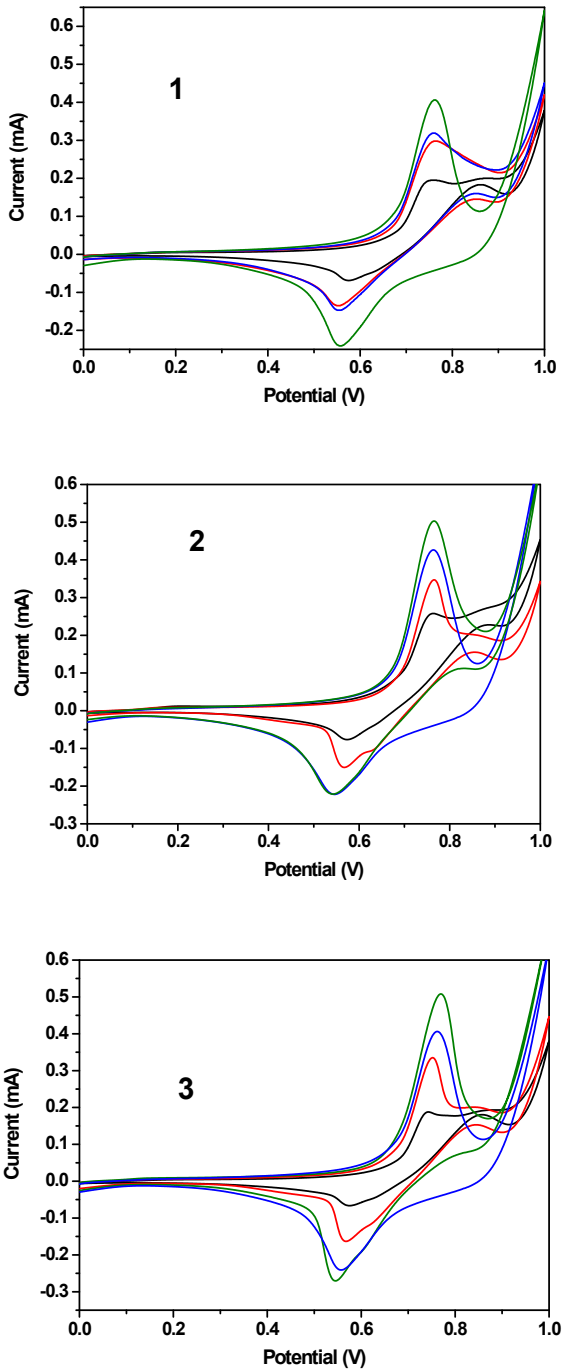

Figure S12. CV runs in real samples without and with urea spiking. In all the samples, the black line shows the response of the real sample without spiking, the red, blue and green line show the response after 0.5, 1.0 and 1.5 mM spiking, respectively.

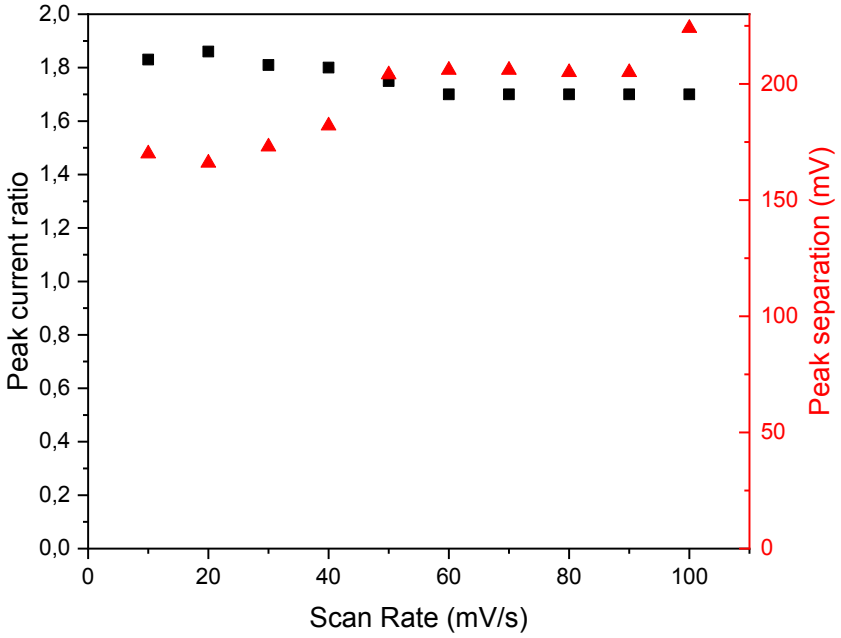

Figure S13: Plot of peak current ratio and separation potential at various scan rates

Table S1: R_S, R_{CT} Q_0 and values for the equivalent circuit reported in figure S11, extracted from the EIS data in the same figure.

Scan rate	Peak current ratio	Peak separation potential
10 mV/s	1.83	170 mV
20 mV/s	1.86	166 mV
30 mV/s	1.81	173 mV
40 mV/s	1.80	182 mV
50 mV/s	1.75	204 mV
60 mV/s	1.70	206 mV
70 mV/s	1.70	206 mV
80 mV/s	1.70	205 mV
90 mV/s	1.70	205 mV
100 mV/s	1.70	224 mV

Table S2: The calculated peak current ratio and separation potential at various scan rates

Sensing nanomaterial	Electrochemical method	Detection limit (μM)	Type	Reference
Nano-tin oxide	CV	600	Enzyme-less	(Ansari et al., 2015)
ZnO NRs	CV	10	Urease based	(Ahmad et al., 2014)
CH–Fe_3O_4/TiO_2	DPV	5000	Urease based	(Kaushik et al., 2009)
TiO_2/Er_2O_3	EIS	3000	Urease based	(Pan et al., 2009)
Vitamin C based NiO	Amperometry	10	Enzyme-less	(Arain et al., 2016)
ZnO nanowire	Amperometry	100	Urease based	(Ali et al., 2011)
Copolymer based ITO	Amperometry	20	Urease based	(Bisht et al., 2005)
$NiCo_2O_4$ NWs/GCE	CV	1	Enzyme-less	Current work

Table S3: Comparison of $NiCo_2O_4$ nanoneedle-modified/GCE non-enzymatic urea sensor with various published works from the literature.